Supplementary Material

Supplementary Figures

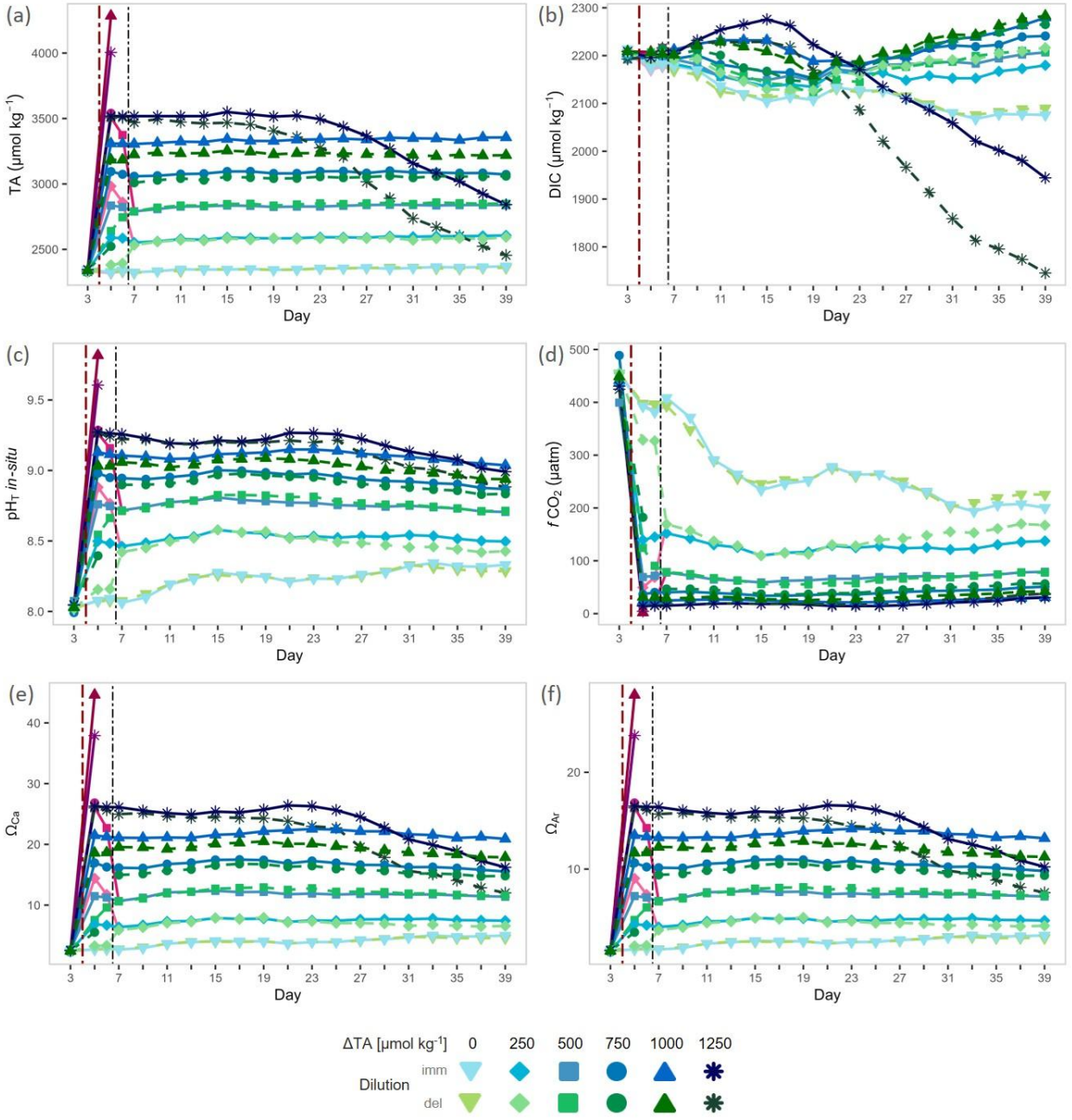

Figure S 1. Temporal variation of carbonate chemistry parameters. *Measured parameters: (a) Total alkalinity (TA), (b) dissolved inorganic carbon (DIC) and (c) pH on total scale (pH_T in-situ). Remaining parameters were calculated with CO2SYS (Pierrot et al., 2021): (d) fugacity of CO_2 (fCO_2), (e) Calcite saturation state (Ω_{Ca}) and (f) Aragonite saturation state (Ω_{Ar}). Water column–averaged temperature and salinity (CTD), as well as dissolved phosphorous and silicate concentrations were used for correction. Carbonate dissociation constants K_1 and K_2 were taken from Lueker et al. (2000). Pink–purple symbols represent surface-layer measurements from delayed-dilution mesocosms on days 5–6; hue encodes the alkalinity addition (ΔTA, µmol kg^{-1}), with darker purple indicating higher ΔTA. The red dash-dotted vertical line marks the start of the alkalinity manipulation; the black dash-dotted line marks completion by mixing via the sediment trap.*

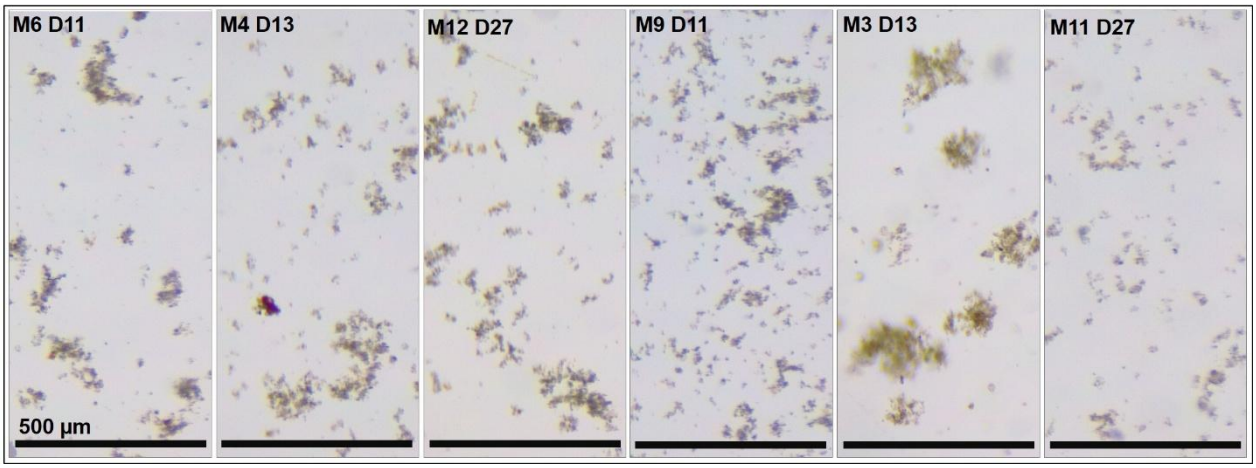

Figure S 2. Particle size structure of sediment trap material. *Light-microscopy images of particulate matter collected from sediment traps of several mesocosms on different sampling days (11, 13, 27), illustrating the range of particle size classes. Panel labels (e.g., "M6 D11") indicate mesocosm identity and day; all images were taken at 400x magnification. Black scale bar = 500 µm.*

(a)

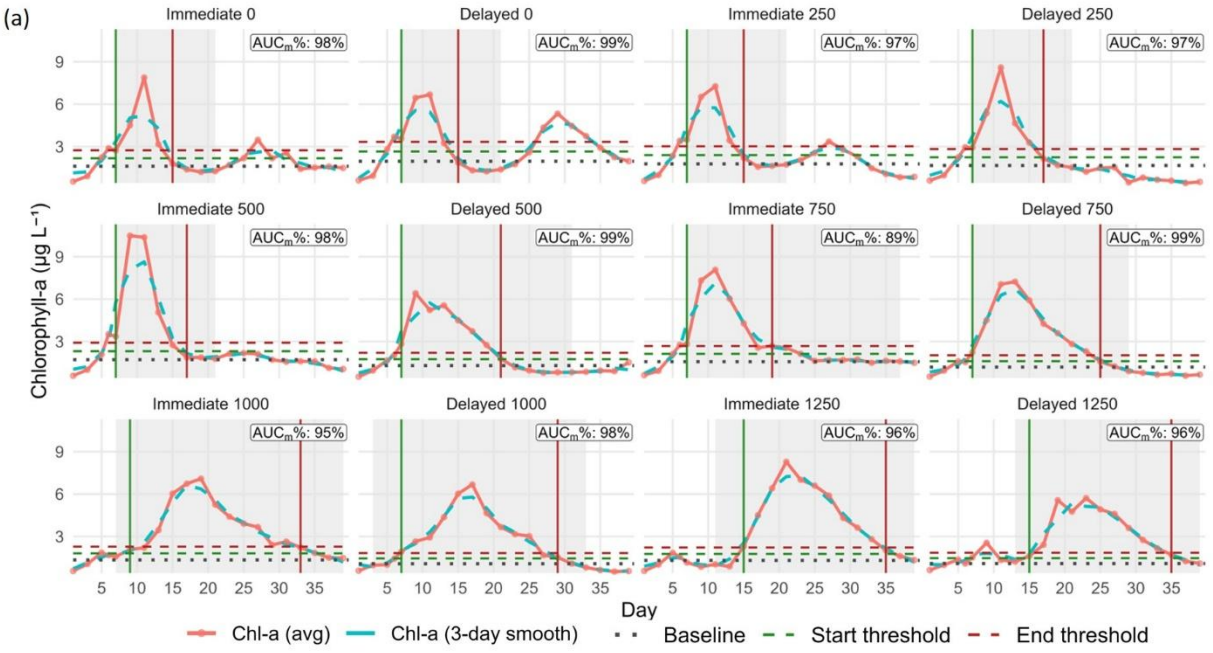

(b)

Mesocosm	Imm 0	Del 0	Imm 250	Del 250	Imm 500	Del 500	Imm 750	Del 750	Imm 1000	Del 1000	Imm 1250	Del 1250
Bloom Start - End [day]	7-15	7-15	7-15	7-17	7-17	7-21	7-19	7-25	9-33	7-29	15-35	15-35
AUC_m%	97.74	99.14	97.17	97.01	97.91	98.51	89.31	98.94	95.07	97.57	96.19	96.21
Baseline [µg L^{-1}]	1.61	1.96	1.77	1.66	1.71	1.29	1.57	1.19	1.34	1.07	1.30	1.09
Threshold Start [µg L^{-1}]	2.17	2.65	2.39	2.24	2.31	1.75	2.13	1.61	1.81	1.45	1.76	1.47
Threshold End [µg L^{-1}]	2.73	3.33	3.01	2.82	2.91	2.20	2.68	2.03	2.28	1.83	2.22	1.85

Figure S 3. Bloom-window detection from Chl a. *(a) Time series per mesocosm with raw Chl-a (salmon) and the 3-day centered smooth (teal). The baseline (B) (black dotted) is the median of smoothed Chl-a on days 1–6. Bloom detection is allowed from day 7 onward and uses asymmetric thresholds to allow hysteresis: Start (green line): first day of a 2-day run where smoothed Chl-a ≥ (1+α*B) and slopes are positive on both days. End (red line, after the global peak): first day of a 2-day run where smoothed Chl-a ≤ (1+β*B) and at least one slope is negative; whereas α = 0.35 and β = 0.70). The grey band marks the reference main-peak window (largest peak bounded by the nearest local minima). AUC_m% in each facet is the area under the smoothed curve and above (B) within the detected bloom window divided by the corresponding area for the reference main peak (trapezoidal integration). (b) Summary table by mesocosm providing bloom start–end days, AUC_m%, baseline (B), and the start/end threshold levels.*

(a)

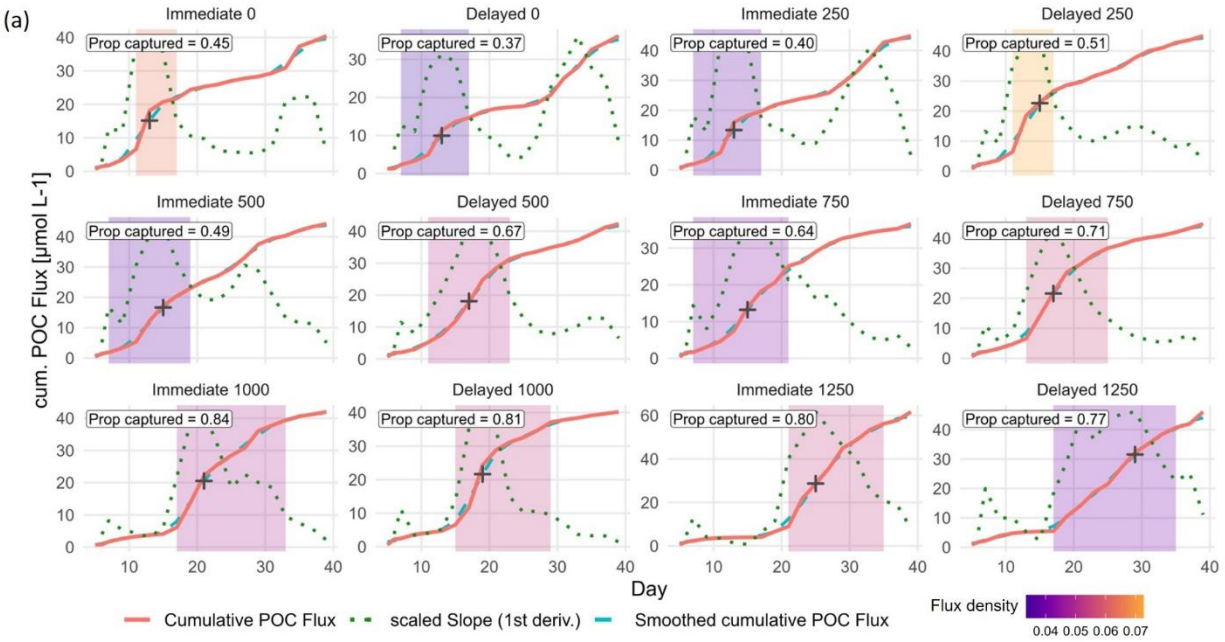

(b)

Mesocosm	Imm 0	Del 0	Imm 250	Del 250	Imm 500	Del 500	Imm 750	Del 750	Imm 1000	Del 1000	Imm 1250	Del 1250
Deposition Start - End [day]	11-17	7-17	7-17	11-17	7-19	11-23	7-21	13-25	17-33	15-29	21-35	17-35
Flux Density [Prop.-captured d^{-1}]	0.064	0.034	0.037	0.072	0.038	0.051	0.043	0.054	0.049	0.053	0.053	0.040
Max. Deposition [day]	13	13	13	15	15	17	15	17	21	19	25	29
Baseline Deposition Intensity (slope) [µmol L^{-1} d^{-1}]	0.20	0.35	0.31	0.35	0.29	0.23	0.21	0.32	0.47	0.35	0.29	0.49
Max. rel. Deposition Intensity (norm. slope) [µmol L^{-1} d^{-1}]	2.68	1.37	2.17	3.03	2.23	2.62	2.06	3.36	2.78	3.37	4.20	1.80
Delay to Bloom Start [day]	4	0	0	4	0	4	0	6	8	8	6	2

Figure S 4. Detection of bloom-following sediment-deposition events from cumulative POC fluxes. *(a) Facets show cumulative POC flux (salmon) with its 3-day centered smooth (teal) and the first derivative ("slope") of the smoothed series (scaled to y-axis, green dotted). Analysis was restricted to a focus window beginning at each mesocosm's water column bloom start and ending at bloom end + extended search window (w). The black + marks the day of maximum relative slope (m_{max}, peak deposition intensity). Relative slopes (m_{rel}) were attained by baseline correction (i.e., subtracting the median of slopes pre-water column bloom (from day5) from daily slopes). Thresholds for start and end of deposition events were determined. Start: day where $m_{rel} \geq \alpha * m_{max}$. End: day where $m_{rel} \leq (1 - \alpha) * m_{max}$ (after m_{max} + water column bloom end). Thresholds used were $\alpha = 0.32$ and $w = 6$ days. Opposing gates for start and end conditions (α vs. $1 - \alpha$) allowed for hysteresis, but kept sensitivities tied. Shaded rectangles depict identified deposition windows and respective flux density (proportion of flux captured per day. Label within facets ("Prop captured") gives the proportion of the total cumulative flux captured. (b) Summary by mesocosm: start–end days, flux density (as proportion captured per day), day of peak deposition, baseline deposition intensity (slope), maximum relative deposition intensity, and the delay of deposition start to bloom start (days). Several combinations of the threshold (α) and the search window (w) were tested to balance coverage (proportion captured) and sharpness (flux density) while matching the observed phenology of cumulative POC flux and slope series. All series use mesocosm-specific bloom windows; methods as in Sect. 2.5.*

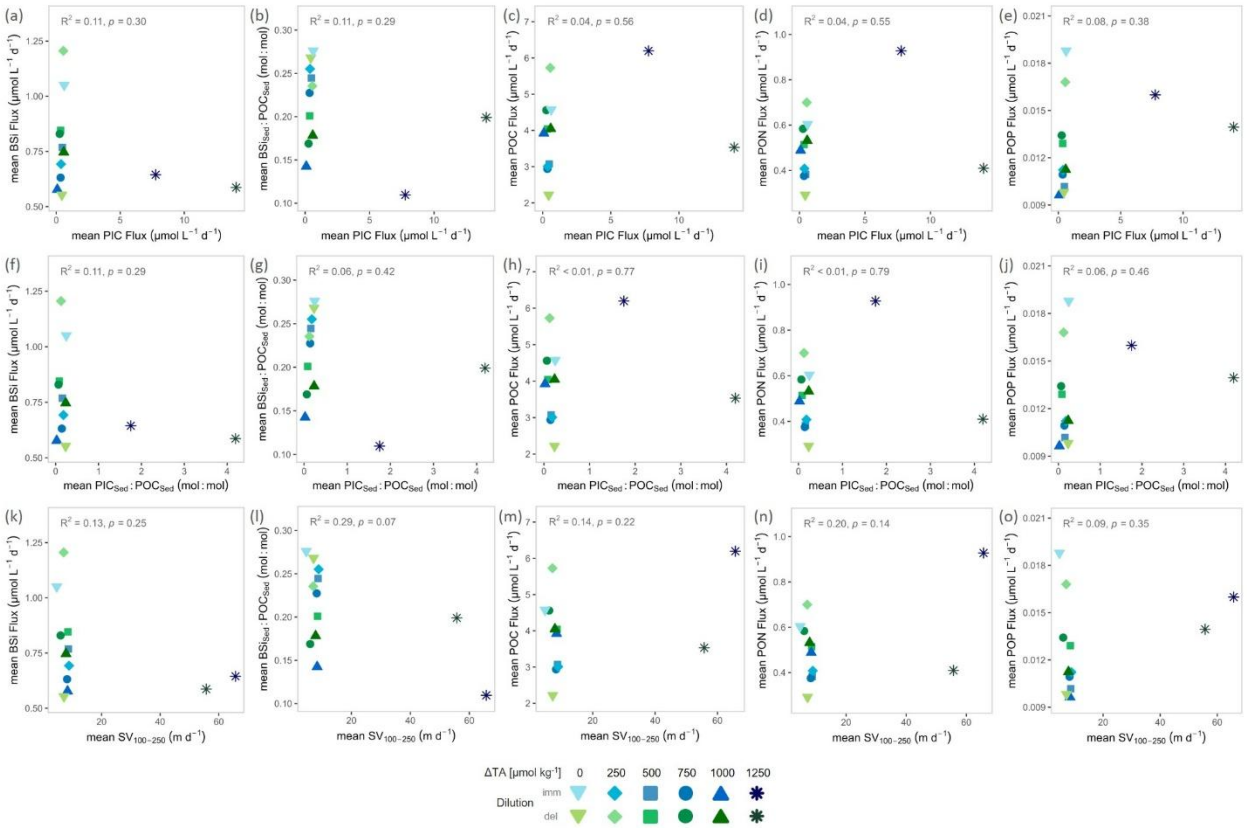

Figure S 5. Carbonate precipitation did not influence organic matter export, stoichiometry or sinking velocities consistently. *Parameter regressions vs. mean particulate inorganic carbon export (PIC Flux): (a) BSi Flux, (b) sediment silica ballasting ratio (BSi_{Sed}:POC_{Sed}), (c) POC Flux, (d) PON Flux, and (e) POP Flux. Parameter regressions vs. mean carbonate ballasting (PIC_{Sed}:POC_{Sed}): (f) BSi Flux, (g) sediment silica ballasting ratio (BSi_{Sed}:POC_{Sed}), (h) POC Flux, (i) PON Flux, and (j) POP Flux. Parameter regressions vs mean particle sinking velocities (in 100-250 µm size class): (k) BSi Flux, (l) sediment silica ballasting ratio (BSi_{Sed}:POC_{Sed}), (m) POC Flux, (n) PON Flux, and (o) POP Flux. All variables are averaged over each mesocosm's deposition window; windows—and thus averaging days—differ among mesocosms (see Sect. 2.5, Fig. S4). Grey annotations report statistical tests (see details in Table S1).*

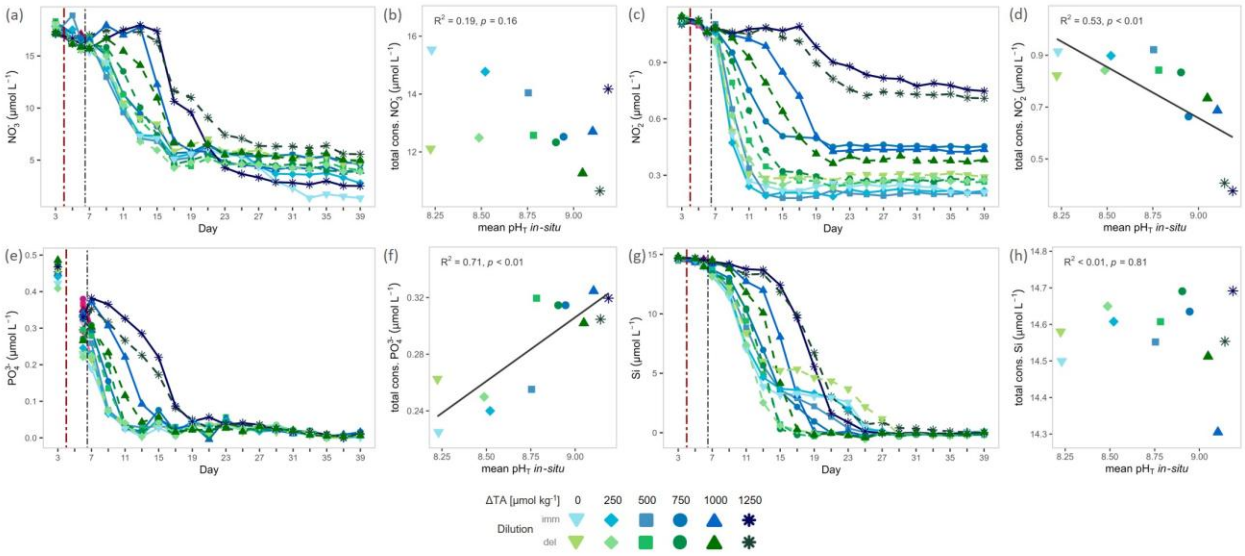

Figure S 6. Temporal variation and total consumption of inorganic nutrients throughout the experiment. *Daily (a) nitrate (NO_3^-), (c) nitrite (NO_2^-), (e) phosphate (PO_4^{3-}) and (f) silicate (Si) concentrations. Total nutrient consumption (b,d,f,h) per species was computed as the absolute decrease in concentration from day 5 to day 39 (PO_4^{3-}: day 6–39) and regressed against the respective window-averaged pH_T. Pink–purple symbols represent surface-layer measurements from delayed-dilution mesocosms on days 5–6; hue encodes the alkalinity addition (ΔTA, µmol kg^{-1}), with darker purple indicating higher ΔTA. The red dash-dotted vertical line marks the start of the alkalinity manipulation; the black dash-dotted line marks completion by mixing via the sediment trap. Grey annotations report statistical tests (see details in Table S1).*

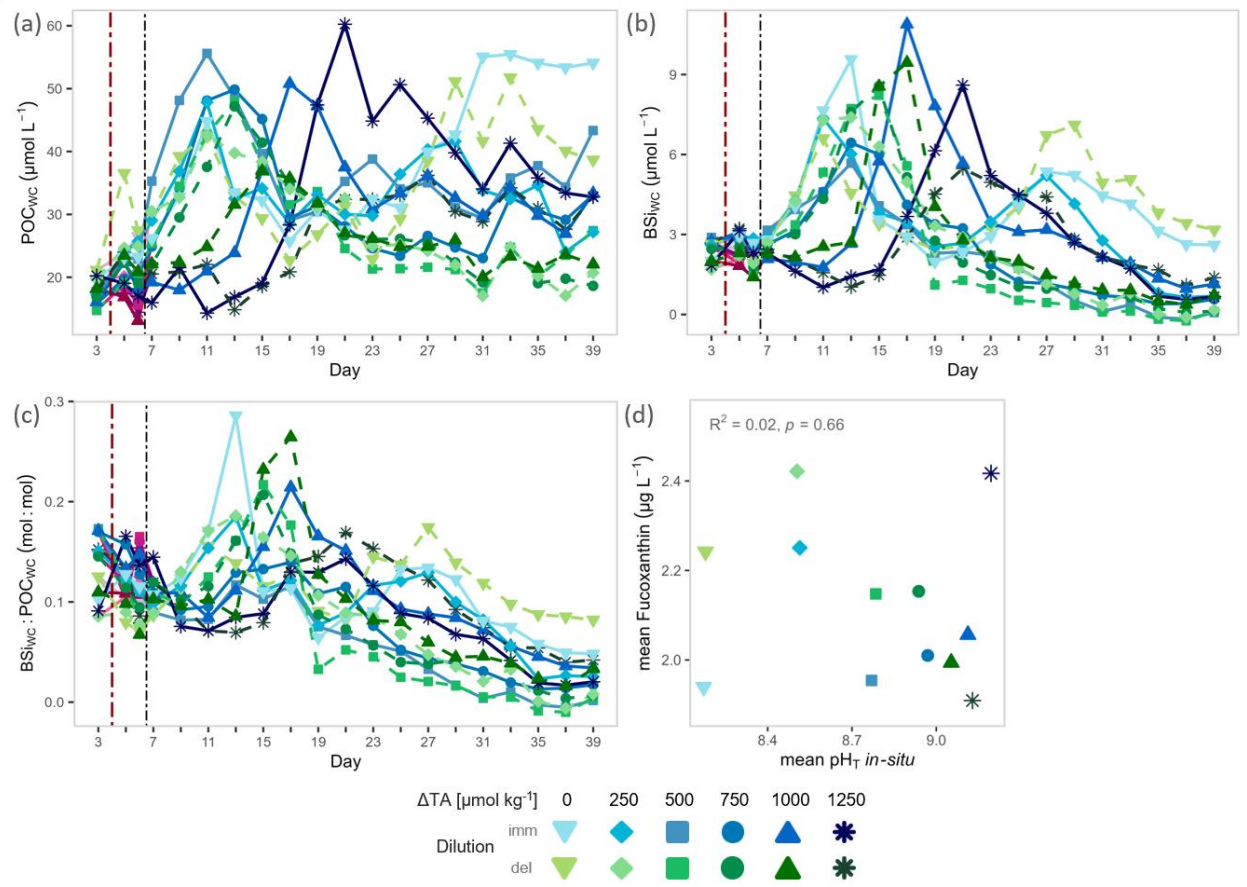

Figure S 7. Temporal variation of water column biomass and stoichiometry. *Daily concentrations of (a) water column particulate organic carbon (POC_{WC}), (b) water column biogenic silica (BSi_{WC}), and daily ratios of (c) water column silicification (BSi_{WC}:POC_{WC}). pH-gradient responses of bloom-window averages for (d) Fucoxanthin. Note: The averaging windows for pH_T and Fucoxanthin differ among mesocosms, defined by the identified bloom window per mesocosm (see Sect. 2.4 and Fig. S3). Pink–purple symbols represent surface-layer measurements from delayed-dilution mesocosms on days 5–6; hue encodes the alkalinity addition (ΔTA, µmol kg^{-1}), with darker purple indicating higher ΔTA. The red dash-dotted vertical line marks the start of the alkalinity manipulation; the black dash-dotted line marks completion by mixing via the sediment trap.*

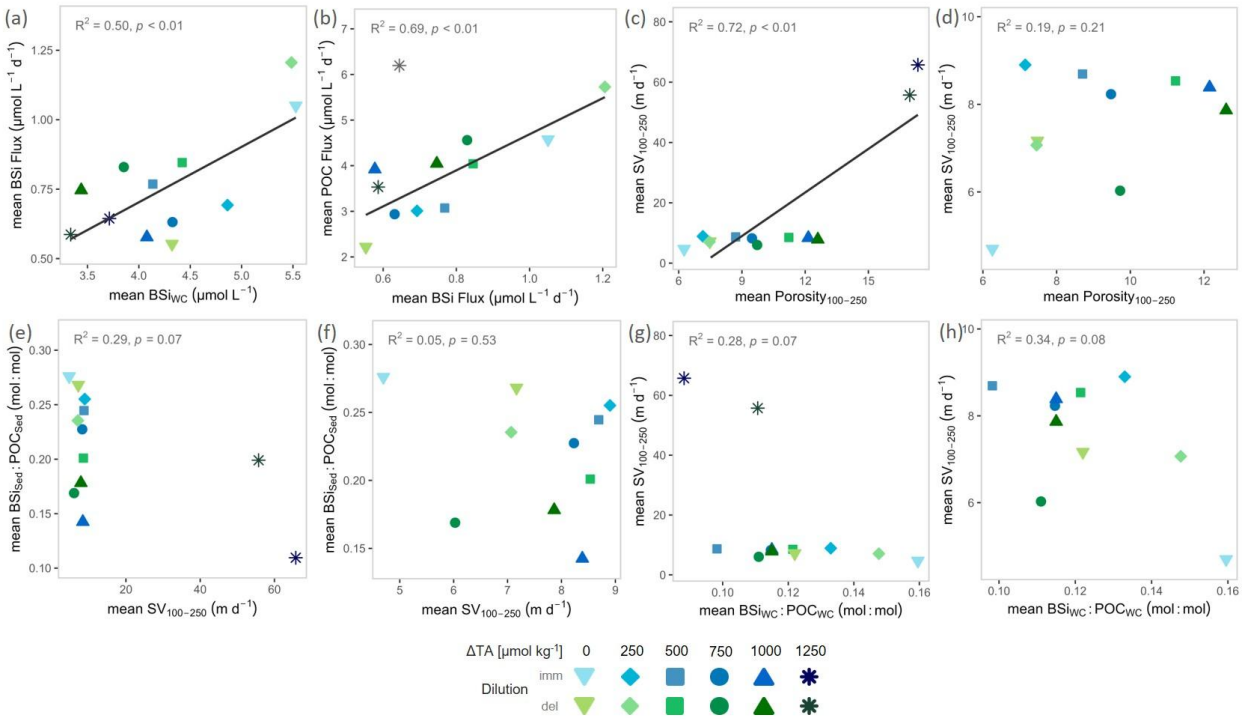

Figure S 8. Links between water-column silica production and export metrics. *Cross-phase regressions (bloom-to-deposition): (a) mean BSi Flux vs. mean BSi_{WC}; (b) mean POC Flux vs. mean BSi Flux. Within-sediment regression: (c-d) mean particle porosity (in 100-250 µm size class) vs. mean particle sinking velocities (in 100-250 µm size class) including and excluding precipitation driven outliers; (e-f) mean BSi_{Sed}:POC_{Sed} vs. mean particle sinking velocities (in 100-250 µm size class) including and excluding precipitation driven outliers and (g-h) mean particle sinking velocities (in 100-250 µm size class) including and excluding precipitation driven outliers vs. mean BSi_{WC}:POC_{WC}. For panel (b) one inconsistent outlier was excluded to clarify respective relationships (grey asterix); results with and without outliers are reported in Table S1. Note: To link processes across phases, sediment parameters (BSi Flux, POC Flux, $SV_{100-250}$) were averaged over each mesocosm's deposition window, whereas the water-column parameters (BSi_{WC}, BSi_{WC}:POC_{WC}) were averaged over each mesocosm's bloom window; for (a) and (g-h) pairs were matched by mesocosm for regression. Both, bloom and deposition windows (and thus averaging days) differ among mesocosms (see Sect. 2.4, 2.5; compare Figs. S3 and S4). Grey annotations report statistical tests (see details in Table S1).*

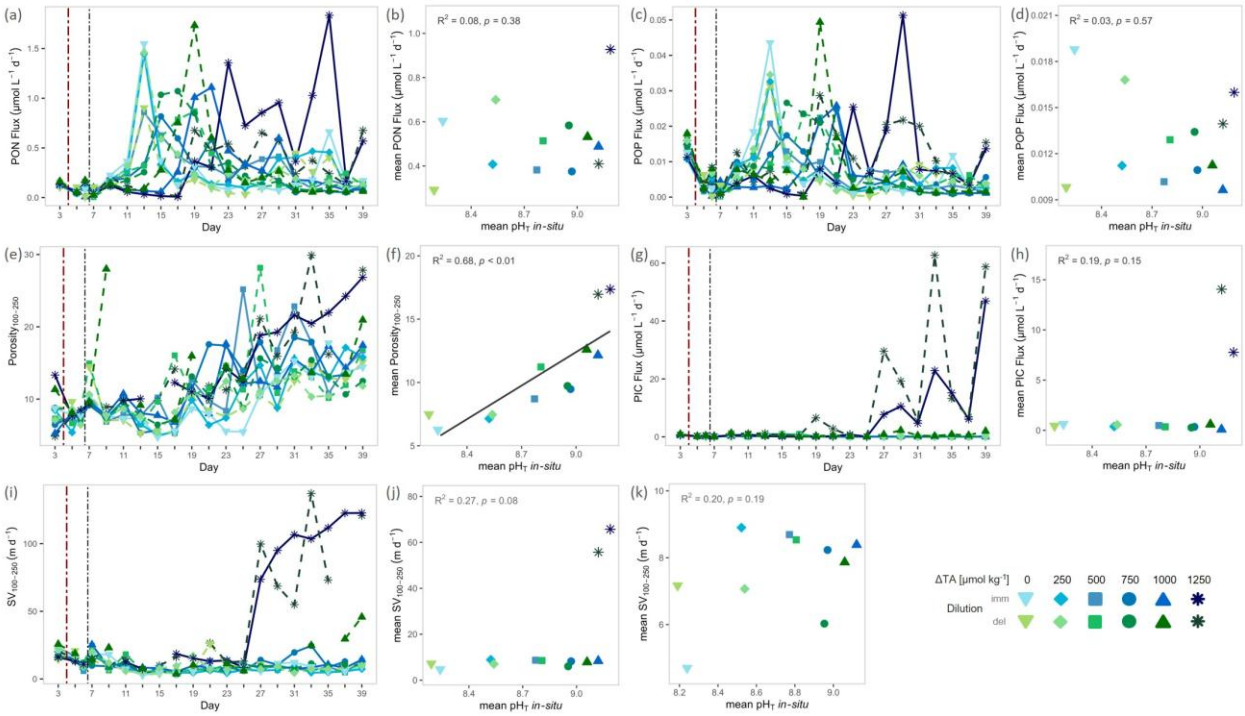

Figure S 9. Sediment export and particle properties during deposition phase. *Temporal trajectories of (a) particulate organic nitrogen export (PON Flux), (c) particulate organic phosphorus export (POP Flux), (e) particle porosity (in 100-250 µm size class), (g) particulate inorganic carbon export (PIC Flux) and (i) particle sinking velocities (in 100-250 µm size class). pH-gradient responses of deposition-window averages of (b) PON Flux, (d) POP Flux, (f) porosity (in 100-250 µm size class), (h) PIC Flux, (j) particle sinking velocities (in 100-250 µm size class) including precipitation driven outliers and (k) particle sinking velocities (in 100-250 µm size class) excluding precipitation driven outliers, plotted against deposition-window mean pH_T. Note: The averaging windows for pH_T and each response variable differ among mesocosms, defined by the identified deposition windows per mesocosm (see Sect. 2.5 and Fig. S4). The red dash-dotted vertical line marks the start of the alkalinity manipulation; the black dash-dotted line marks completion by mixing via the sediment trap. Grey annotations report statistical tests (see Table S1).*

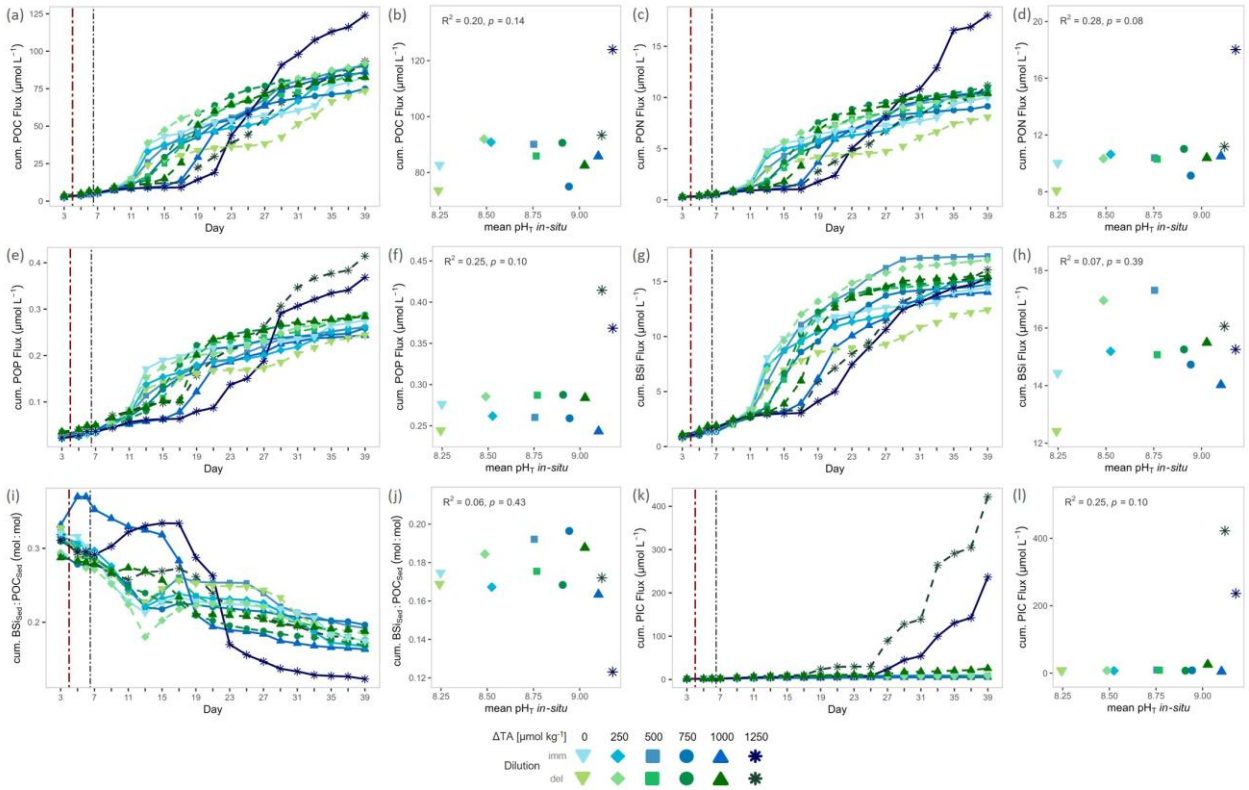

Figure S 10. Cumulative particulate export and stoichiometry under OAE. *Temporal trajectories of cumulative fluxes for (a) POC Flux, (c) PON Flux, (e) POP Flux, (g) BSi Flux, (i) sediment silica ballasting ratios (BSi_{Sed}:POC_{Sed}), and (k) PIC Flux. pH-gradient responses: for each mesocosm, the cumulative value at day 39 (from corresponding time series) is regressed against the mean pH_T averaged over days 5–39. The red dash-dotted vertical line marks the start of the alkalinity manipulation; the black dash-dotted line marks completion by mixing via the sediment trap. Grey annotations report statistical tests (see Table S1).*

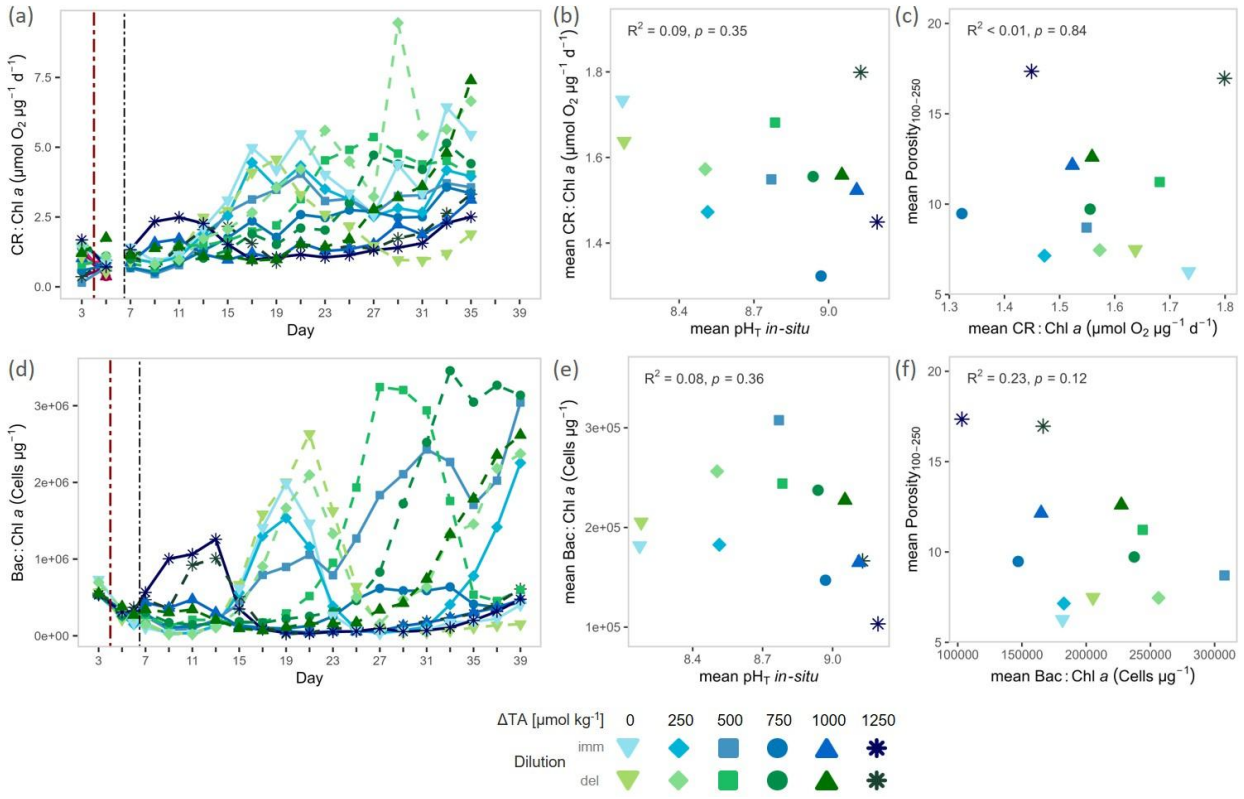

Figure S 11. Community respiration and bacteria abundances normalized to phytoplankton biomass. *Temporal trajectories of (a) chlorophyll a normalized community respiration (CR:Chl a) and (c) chlorophyll a normalized bacterial abundances (Bac:Chl a). pH-gradient responses: bloom-window averages of (b) CR:Chl a and (d) Bac:Chl a plotted against the corresponding bloom-window mean pH_T. Cross-phase regressions (bloom-to-deposition): (c) mean $Porosity_{100\text{-}250}$ vs. mean CR:Chl a; (f) mean $Porosity_{100\text{-}250}$ vs. mean Bac:Chl a. Note: To link processes across phases, sediment parameters ($Porosity_{100\text{-}250}$) were averaged over each mesocosm's deposition window, whereas the water-column parameters (CR:Chl a, Bac:Chl a) was averaged over each mesocosm's bloom window; for (b-c, and e-f) pairs were matched by mesocosm for regression. Both, bloom and deposition windows (and thus averaging days) differ among mesocosms (see Sect. 2.4, 2.5; compare Figs. S3 and S4). Grey annotations report statistical tests (see details in Table S1). Pink–purple symbols represent surface-layer measurements from delayed-dilution mesocosms on days 5–6; hue encodes the alkalinity addition (ΔTA, µmol kg^{-1}), with darker purple indicating higher ΔTA. The red dash-dotted vertical line marks the start of the alkalinity manipulation; the black dash-dotted line marks completion by mixing via the sediment trap. Grey annotations report statistical tests (see details in Table S1).*

Supplementary Table S1

Table S 1: Linear regression models describing relationships between alkalinity treatments (expressed as pH_T) and water-column as well as export responses. *All predictors and response variables were treated as continuous. Data exclusions, where applied, are indicated in the table and highlighted in the corresponding figures. Models are grouped by figure to support Figures 2–4 and Supplementary Figures S2, S4, S6–S10. For each model, intercepts, slopes, coefficients of determination (R^2), and p-values are reported.*

	Datasets	Intercept	Slope	R^2	p-value
Fig. 2	pH_T – Chl *a*	5.76	-0.1605	< 0.01	0.7627
	pH_T – POC_{WC}	46.51	-1.3102	0.013	0.7257
	pH_T – BSi_{WC}	17.84	-1.5437	0.61	**0.0027**
	pH_T – BSi_{WC}:POC_{WC}	0.48	-0.0409	0.56	**0.0051**
Fig. 3	pH_T – POC Flux	-4.13	0.9238	0.075	0.3881
	pH_T – BSi Flux	2.83	-0.2352	0.166	0.189
	pH_T – BSi_{Sed}:POC_{Sed}	1.34	-0.1289	0.738	**0.0003**
Fig. 4	$Porosity_{100\text{-}250}$ – BSi_{Sed}:POC_{Sed}	0.33	-0.0113	0.641	**0.0018**
	BSi_{WC}:POC_{WC} – Bsi_{Sed}:POC_{Sed}	< 0.01	1.7293	0.429	**0.0207**
Fig. S2	pH_T – cons. NO_3^-	28.95	-1.8248	0.189	0.1576
	pH_T – cons. NO_2^-	4.20	-0.3941	0.529	**0.0074**
	pH_T – cons. PO_4^{3-}	-0.51	0.0901	0.712	**0.0006**
	pH_T – cons. Si	14.79	-0.0243	0.006	0.8080
Fig. S4	pH_T – Fucoxanthin	2.75	-0.0711	0.021	0.6567
Fig. S6	pH_T – PON Flux	-0.70	0.1383	0.076	0.3844
	pH_T – POP Flux	0.03	-0.0016	0.034	0.5657
	pH_T – $Porosity_{100\text{-}250}$	-66.95	8.8165	0.683	**0.0009**
	pH_T – PIC Flux	-46.19	5.5003	0.194	0.1516
	pH_T – $SV_{100\text{-}250}$	-258.66	31.2939	0.268	0.0848
	pH_T – $SV_{100\text{-}250}$ (excl. outliers)	-8.33	1.8224	0.202	0.1923
Fig. S7	pH_T – cum. POC Flux	-64.19	17.4397	0.205	0.1399
	pH_T – cum. PON Flux	-22.90	3.8449	0.278	0.0779
	pH_T – cum. POP Flux	-0.39	0.0770	0.248	0.0994
	pH_T – cum. BSi Flux	5.88	1.0602	0.074	0.3928
	pH_T – cum. BSi_{Sed}:POC_{Sed}	0.30	-0.0144	0.064	0.4280
	pH_T – cum. PIC Flux	-1669.03	197.3797	0.250	0.0978
Fig. S8	PIC Flux – BSi Flux	0.79	-0.015	0.106	0.3026
	PIC Flux – BSi_{Sed}:POC_{Sed}	0.22	-0.004	0.113	0.2858
	PIC Flux – POC Flux	3.88	0.0509	0.036	0.5571
	PIC Flux – PON Flux	0.50	0.0078	0.037	0.5468
	PIC Flux – POP Flux	0.01	0.0002	0.077	0.3812
	PIC_{Sed}:POC_{Sed} – BSi Flux	0.79	-0.0541	0.11	0.2934
	PIC_{Sed}:POC_{Sed} – BSi_{Sed}:POC_{Sed}	0.22	-0.0108	0.065	0.4239
	PIC_{Sed}:POC_{Sed} – POC Flux	3.93	0.0918	0.009	0.7657
	PIC_{Sed}:POC_{Sed} – PON Flux	0.51	0.0122	0.007	0.7901
	PIC_{Sed}:POC_{Sed} – POP Flux	0.01	0.0006	0.057	0.4554
	$SV_{100\text{-}250}$ – BSi Flux	0.82	-0.0035	0.131	0.2485
	$SV_{100\text{-}250}$ – BSi_{Sed}:POC_{Sed}	0.23	-0.0013	0.288	0.0717
	$SV_{100\text{-}250}$ – POC Flux	3.64	0.0211	0.144	0.2244
	$SV_{100\text{-}250}$ – PON Flux	0.46	0.0037	0.203	0.1411
	$SV_{100\text{-}250}$ – POP Flux	0.01	< 0.0001	0.087	0.3529

Fig. S9	BSi_{WC} – BSi Flux	-0.10	0.1995	0.505	**0.0096**
	BSi Flux – POC Flux (excl. outlier)	0.74	3.9528	0.694	**0.0015**
	$Porosity_{100\text{-}250}$ – $SV_{100\text{-}250}$	-34.34	4.8136	0.722	**0.0005**
	$Porosity_{100\text{-}250}$ – $SV_{100\text{-}250}$ (excl. outliers)	5.14	0.2620	0.186	0.2134
	$SV_{100\text{-}250}$ – BSi_{Sed}:POC_{Sed}	0.23	-0.0013	0.288	0.0717
	$SV_{100\text{-}250}$ – BSi_{Sed}:POC_{Sed} (excl. outliers)	0.28	-0.0077	0.052	0.5270
	BSi_{WC}:POC_{WC} – $SV_{100\text{-}250}$	84.16	-565.9188	0.283	0.0748
	BSi_{WC}:POC_{WC} – $SV_{100\text{-}250}$ (excl. outliers)	12.88	-43.0350	0.342	0.0756
Fig. S10	pH_T – CR:Chl *a*	2.51	-0.1074	0.089	0.3473
	CR:Chl *a* – $Porosity_{100\text{-}250}$	7.53	1.9157	0.005	0.8351
	pH_T – Bac:Chl *a*	597584.36	-45070.6675	0.085	0.3587
	Bac:Chl *a* – $Porosity_{100\text{-}250}$	16.89	< 0.0001	0.226	0.1187